

Analytical correlations for intermediate temperature PEM fuel cells

Denver Cheddie*, Norman Munroe

*Mechanical and Materials Engineering, CEAS 2103, Florida International University,
10555 W Flagler Street, Miami, FL 33174, United States*

Received 17 November 2005; received in revised form 8 January 2006; accepted 11 January 2006

Available online 21 February 2006

Abstract

This paper presents analytical correlations, which predict the polarization performance and thermal effects in an intermediate temperature proton exchange membrane fuel cell (PEMFC). Such correlations are useful for engineers and designers of fuel cells to expedite calculations without depending on complex computational models. Analytical results compare well with published experimental polarization data. They also indicate the temperature variations and dominant modes of heat transfer in a unit cell.

© 2006 Elsevier B.V. All rights reserved.

Keywords: Analytical correlations; Intermediate temperature; Fuel cell

1. Introduction

Low temperature (<90 °C) proton exchange membrane fuel cells (PEMFCs) have long been considered as candidates for future energy systems. However, numerous debilitating factors – such as sluggish electrode kinetics, susceptibility of platinum (Pt) catalysts to CO poisoning, and water management problems associated with Nafion® membranes – have hindered their progress.

Much research has been conducted on new proton conducting membranes that are capable of operating at intermediate temperatures (150–200 °C) [1]. At these temperatures CO poisoning becomes less prominent, electrode kinetics are faster, and water would exist primarily in the vapor phase precluding problems associated with water management and mass transport limitations.

Although modeling of PEMFCs has received much attention over the past 15 years [2], most of the work is based on PEMFCs using a Nafion® membrane. In a previous paper [3], we developed a mathematical model for a PEMFC using a polybenzimidazole (PBI) membrane. Mathematical models, however, tend to be very complex and esoteric, and do not parametrically illustrate the dependence of the final solution on factors affecting

it. They provide detailed and accurate calculations for complex designs, however, analytical correlations, even if approximate, enable quick calculations for most engineering purposes.

This paper presents correlations based on analytical solutions for the model of the PBI PEMFC developed in ref. [3]. The analytical results are compared to the experimental results published by Wang et al. [4].

2. Mathematical formulation

The domain of interest is the membrane electrode assembly (MEA). For the purpose of a 1D study, the gas flow channels are not considered; instead boundary conditions are derived at the gas channel/gas diffuser interfaces. Fig. 1 shows the schematic of the membrane electrode assembly (MEA) and the dimensionless coordinates used.

Only steady state operation is considered, and at 150 °C, water is expected to exist only in the vapor phase, and all electrochemical reactions occur in the gaseous phase. The gas diffuser regions are modeled as macro-homogenous porous media. The catalyst is treated as an interface, where species are consumed and produced.

2.1. Equations

The phenomenological equations, based on the Stefan–Maxwell equations, Darcy’s law, conservation laws,

* Corresponding author. Tel.: +1 786 877 9235; fax: +1 305 348 1932.

E-mail addresses: dcheddie@yahoo.com (D. Cheddie),
Norman.Munroe@arc.fiu.edu (N. Munroe).

Nomenclature

A	MEA cross sectional area
c	specific heat capacity
D	gas pair diffusivity
E	potential
F	Faraday constant, $96,487 \text{ C mol}^{-1}$
I	current density
k	thermal conductivity
l	thickness
m	mass fraction
M	molecular mass
N	mass flux
P	pressure
R	universal gas constant, $8.3143 \text{ J mol}^{-1} \text{ K}^{-1}$
S	source, entropy
T	temperature
u	mass averaged velocity
V	volumetric flow rate, potential

Greek letters

α	charge transfer co-efficient
β	porous media gas permeability
ε	gas porosity
μ	dynamic viscosity
ρ	density
σ	conductivity

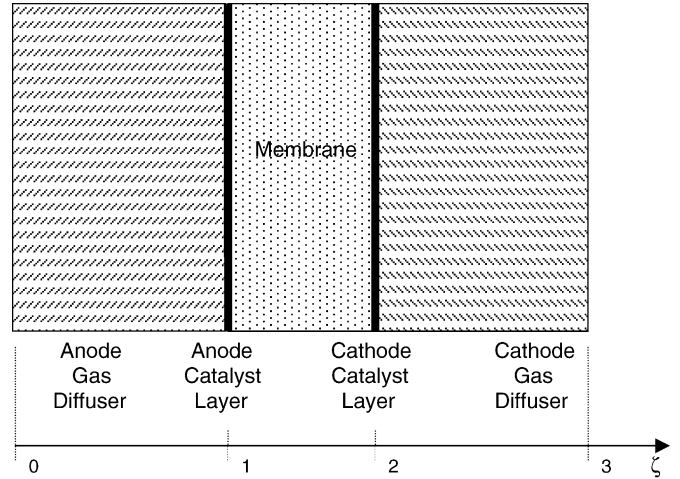


Fig. 1. Schematic of the MEA with dimensionless coordinates.

The entropy change term for the overall fuel cell reaction with water in the vapor form is correlated using thermodynamics tables. The following relation is valid for $400 \text{ K} < T < 500 \text{ K}$

$$\frac{\Delta S}{n} = -18.449 - 0.01283T \text{ J mol}^{-1} \text{ K}^{-1} \quad (3)$$

The activation overpotential at the cathode catalyst layer is calculated from the Tafel relation

$$E_{\text{act}} = \frac{RT}{2\alpha F} \ln \left(\frac{I}{I_0} \right) \quad (4)$$

The anode overpotential is neglected since at elevated temperatures, the electrode kinetics associated with hydrogen dissociation is expected to be much faster than for oxygen reduction. The total ohmic overpotential is given by

$$E_{\text{ohm}} = I \left(\frac{l_m}{\sigma_m} + \frac{2l_d}{\sigma_d^{\text{eff}}} \right) \quad (5)$$

The operating cell potential is given by the reversible potential (concentration effects included) less the activation and ohmic overpotentials

$$E_{\text{cell}} = E_r - E_{\text{act}} - E_{\text{ohm}} \quad (6)$$

The energy equation over the entire unified domain is given by Eq. (7), which accounts for convection, conduction and heat

and ideal gas laws, are shown in Table 1, as derived in ref. [3].

Once the partial pressures of hydrogen, oxygen and vapor at their respective catalyst layers are determined, the reversible cell potential at a given temperature can be calculated from Eq. (1). The reversible cell potential at T_{ref} ($=298 \text{ K}$) is 1.185 V for water existing in the vapor phase

$$E_r = E_r^0 + \frac{\Delta S}{nF}(T - T_{\text{ref}}) + \frac{2RT}{nF} \ln \left(\frac{p_{\text{H}_2} \times p_{\text{O}_2}^{0.5}}{p_w} \right) \quad (1)$$

where

$$p_i = P \frac{m_i/M_i}{\sum m_i/M_i} \quad (2)$$

Table 1
Summary of governing equations

	Anode	Cathode
Fluxes	$N_{\text{H}_2} = \frac{IM_{\text{H}_2}}{2F}, N_w = 0$	$N_{\text{O}_2} = -\frac{IM_{\text{O}_2}}{4F}, N_w = \frac{IM_w}{2F}, N_{\text{N}_2} = 0$
Species conservation	$\frac{dm_{\text{H}_2}}{dz} = -\frac{N_{\text{H}_2}}{\rho D_{\text{O}_2, \text{H}_2}^{\text{eff}}} (1 - m_{\text{H}_2}), m_w = 1 - m_{\text{H}_2}$	$\frac{dm_{\text{O}_2}}{dz} = \frac{1}{\rho} \left(\frac{-m_{\text{N}_2} N_{\text{O}_2}}{D_{\text{O}_2, \text{N}_2}^{\text{eff}}} + \frac{m_{\text{O}_2} N_w - m_w N_{\text{O}_2}}{D_{w, \text{O}_2}^{\text{eff}}} \right), \frac{dm_{\text{N}_2}}{dz} = \frac{1}{\rho} \left(\frac{m_{\text{N}_2} N_w}{D_{w, \text{N}_2}^{\text{eff}}} + \frac{m_{\text{N}_2} N_{\text{O}_2}}{D_{\text{O}_2, \text{N}_2}^{\text{eff}}} \right),$ $m_w = 1 - m_{\text{O}_2} - m_{\text{N}_2}$
Ideal gas relation	$\rho = \frac{P}{RT} \left(\frac{m_{\text{H}_2}}{M_{\text{H}_2}} + \frac{m_w}{M_w} \right)^{-1}$	$\rho = \frac{P}{RT} \left(\frac{m_{\text{O}_2}}{M_{\text{O}_2}} + \frac{m_{\text{N}_2}}{M_{\text{N}_2}} + \frac{m_w}{M_w} \right)^{-1}$
Mass conservation	$\rho u = N_{\text{H}_2} + N_w = \frac{IM_{\text{H}_2}}{2F}$	$\rho u = N_{\text{O}_2} + N_{\text{N}_2} + N_w = \frac{I}{4F} (2M_w - M_{\text{O}_2})$
Darcy's law	$\frac{dP}{dz} = -\frac{\mu}{\beta} u$	$\frac{dP}{dz} = -\frac{\mu}{\beta} u$

generation. In the membrane, since there is no fluid flow, the convection term vanishes

$$\rho u \frac{d(cT)}{dz} = k_{\text{eff}} \frac{d^2 T}{dz^2} + S_T \quad (7)$$

The heat generation is due to ohmic heating and heat of reaction

$$S_T = S_{\text{ohmic}} + S_{\text{reaction}} \quad (8)$$

$$S_{\text{ohmic}} = \frac{I^2}{\sigma} \quad (9)$$

The heat of reaction is considered to be concentrated in the cathode catalyst layer. It is due to the entropy of reaction and the irreversibility associated with activation overpotential

$$S_{\text{reaction}} = I \left(E_{\text{act}} - \frac{T\Delta S}{nF} \right) \quad (10)$$

2.2. Boundary conditions

At the interface of the gas flow channel and gas diffusers, the mass fraction boundary conditions can be determined from a material balance between gas supply and reaction requirements

$$\text{at } \zeta = 0, \quad m_{\text{H}_2}^0 = \frac{m_{\text{H}_2, \text{IN}}^0 - A_{\text{xs}} N_{\text{H}_2}}{(m_{\text{H}_2, \text{IN}}^0 - A_{\text{xs}} N_{\text{H}_2}) + (m_{\text{w}, \text{IN}}^0)} \quad (11)$$

at $\zeta = 3$,

$$m_{\text{O}_2}^0 = \frac{m_{\text{O}_2, \text{IN}}^0 - A_{\text{xs}} |N_{\text{O}_2}|}{(m_{\text{O}_2, \text{IN}}^0 - A_{\text{xs}} |N_{\text{O}_2}|) + (m_{\text{N}_2, \text{IN}}^0) + (m_{\text{w}, \text{IN}}^0 + A_{\text{xs}} |N_{\text{w}}|)} \quad (12)$$

at $\zeta = 3$,

$$m_{\text{N}_2}^0 = \frac{m_{\text{N}_2, \text{IN}}^0}{(m_{\text{N}_2, \text{IN}}^0 - A_{\text{xs}} |N_{\text{O}_2}|) + (m_{\text{N}_2, \text{IN}}^0) + (m_{\text{w}, \text{IN}}^0 + A_{\text{xs}} |N_{\text{w}}|)} \quad (13)$$

Since each gas occupies the same volume, the inlet mass flow rate for each species can be calculated from Eq. (14)

$$m_{i, \text{IN}}^0 = \frac{p_i M_i V_{\text{IN}}^0}{RT} \quad (14)$$

The temperature at which supply gases are humidified determines the partial pressure of the water vapor. The partial pressures of oxygen and nitrogen are determined from the stoichiometric make up of air (21% oxygen, 79% atmospheric nitrogen by molar composition).

The boundary conditions for the temperature and pressure are set to the supply temperatures and pressures at the interfaces between the gas flow channels and the gas diffusers. At the interfaces, continuity of all variables is specified.

2.3. Analytical solutions

It can be shown that the solution of the general ordinary differential equation

$$\frac{dy(x)}{dx} = A(x)(B + Cy)(D + Ey) \quad (15)$$

with boundary condition $y(x_1) = y_1$, and $DC \neq BE$, is

$$y = \frac{DH - B}{C - EH} \quad (16)$$

where

$$H = \frac{B + Cy_1}{D + Ey_1} \exp[(DC - BE)\bar{A}(x - x_1)] \quad (17)$$

$$\bar{A}(x - x_1) = \int_{x_1}^x A(\chi) d\chi \quad (18)$$

The Stefan–Maxwell equation can be combined with the ideal gas relationship to obtain an ODE similar to Eq. (15)

$$\begin{aligned} \frac{dm_{\text{H}_2}}{dz} = & -\frac{N_{\text{H}_2} RT(z)}{M_{\text{H}_2} D_{\text{w}, \text{H}_2}^{\text{eff}} P_a} \\ & \times \left[\frac{M_{\text{H}_2}}{M_w} + \left(1 - \frac{M_{\text{H}_2}}{M_w}\right) m_{\text{H}_2} \right] [1 - m_{\text{H}_2}] \end{aligned} \quad (19)$$

It is assumed that due to the low viscosity of the gas phases, the pressure drops will be negligible. The mass fraction of hydrogen at the anode catalyst layer becomes

$$m_{\text{H}_2}^{\text{ac}} = \frac{H - (M_{\text{H}_2}/M_w)}{1 - (M_{\text{H}_2}/M_w) + H} \quad (20)$$

$$\begin{aligned} H = & \frac{(M_{\text{H}_2}/M_w) + (1 - (M_{\text{H}_2}/M_w))m_{\text{H}_2}^0}{1 - m_{\text{H}_2}^0} \\ & \times \exp\left(-\frac{IRT_a l_d}{2FD_{\text{w}, \text{H}_2} P_a}\right) \end{aligned} \quad (21)$$

In the cathode gas diffuser, there are two dependent species variables. For simplification, it will be assumed that the mass fraction of nitrogen remains approximately constant. Species flow under the influence of a total pressure gradient (convection) and a concentration gradient (diffusion). Since the total pressure gradient is expected to be negligible, the concentration gradient becomes the dominant factor affecting species flux. Also, since there is no net flux of the inert nitrogen species in the MEA, its concentration or partial pressure gradient is negligible. Hence, the mass fraction is expected to be approximately constant.

The corresponding equation in the cathode gas diffuser is

$$\begin{aligned} \frac{dm_{\text{O}_2}}{dz} = & \frac{N_{\text{O}_2} RT(z)}{M_{\text{O}_2} D_{\text{w}, \text{O}_2}^{\text{eff}} P_c} \left[\left(\frac{M_{\text{O}_2}}{M_{\text{N}_2}} - \frac{M_{\text{O}_2}}{M_{\text{w}_2}} \right) m_{\text{N}_2}^0 + \frac{M_{\text{O}_2}}{M_{\text{w}_2}} \right. \\ & + \left(1 - \frac{M_{\text{O}_2}}{M_w}\right) m_{\text{O}_2} \left. \right] \left[\left(1 - \frac{D_{\text{w}, \text{O}_2}}{D_{\text{N}_2, \text{O}_2}}\right) m_{\text{N}_2}^0 - 1 \right. \\ & \left. + \left(\frac{N_w}{N_{\text{O}_2}} + 1 \right) m_{\text{O}_2} \right] \end{aligned} \quad (22)$$

the solution of which, is

$$m_{\text{O}_2}^{\text{cc}} = \frac{DH - B}{C - EH} \quad (23)$$

where

$$\bar{A} = -\frac{IR\bar{T}_c}{4FD_{\text{w},\text{O}_2}^{\text{eff}}P_c} \quad (24)$$

$$B = \left(\frac{M_{\text{O}_2}}{M_{\text{N}_2}} - \frac{M_{\text{O}_2}}{M_{\text{w}_2}}\right)m_{\text{N}_2}^0 + \frac{M_{\text{O}_2}}{M_{\text{w}_2}} \quad (25)$$

$$C = 1 - \frac{M_{\text{O}_2}}{M_{\text{w}}} \quad (26)$$

$$D = \left(1 - \frac{D_{\text{w},\text{O}_2}}{D_{\text{N}_2,\text{O}_2}}\right)m_{\text{N}_2}^0 - 1 \quad (27)$$

$$E = 1 - 2\frac{M_{\text{w}}}{M_{\text{O}_2}} \quad (28)$$

$$H = \frac{B + Cm_{\text{O}_2}^0}{D + Em_{\text{O}_2}^0} \exp[(BE - CD)\bar{A}l_d] \quad (29)$$

$$m_{\text{w}}^{\text{cc}} = 1 - m_{\text{O}_2}^{\text{cc}} - m_{\text{N}_2}^0 \quad (30)$$

The partial pressures necessary to determine the cell potential can now be found

$$p_{\text{H}_2} = \frac{m_{\text{H}_2}^{\text{ac}}/M_{\text{H}_2}}{(m_{\text{H}_2}^{\text{ac}}/M_{\text{H}_2}) + (1 - m_{\text{H}_2}^{\text{ac}}/M_{\text{w}})P_0} P_a \quad (31)$$

$$p_{\text{O}_2} = \frac{m_{\text{O}_2}^{\text{cc}}/M_{\text{O}_2}}{(m_{\text{O}_2}^{\text{cc}}/M_{\text{O}_2}) + (m_{\text{N}_2}^0/M_{\text{N}_2}) + (m_{\text{w}}^{\text{cc}}/M_{\text{w}})P_0} P_c \quad (32)$$

$$p_{\text{w}} = \frac{m_{\text{w}}^{\text{cc}}/M_{\text{w}}}{(m_{\text{O}_2}^{\text{cc}}/M_{\text{O}_2}) + (m_{\text{N}_2}^0/M_{\text{N}_2}) + (m_{\text{w}}^{\text{cc}}/M_{\text{w}})P_0} P_c \quad (33)$$

All the required parameters are available at this point, except the average temperature in each diffuser region. For a simplified analysis, the temperature variation (in K) could be considered negligible, in which case, \bar{T} could be replaced by T_0 in Eqs. (21) and (24).

It is still desired though to perform a detailed thermal analysis. The energy equation consists of conduction, convection, and generation terms. The generation term can be broken up into ohmic heating (volumetric) and heat of reaction (interfacial). Also of note is that in the membrane, there is no fluid flow, hence the convection term vanishes. In a given domain with BCs, $T(0) = T_i$ and $T(L) = T_0$, the analytical solution of the energy equation is

$$T = T_i + \frac{B}{A}z + \left[\frac{A(T_0 - T_i) - BL}{A}\right] \times \left[\frac{\exp(Az) - 1}{\exp(AL) - 1}\right] \quad (34)$$

$$\frac{dT}{dz} = \frac{B}{A} + [A(T_0 - T_i) - BL] \times \left[\frac{\exp(Az)}{\exp(AL) - 1}\right] \quad (35)$$

where

$$A = \frac{\rho uc}{k} \quad (36)$$

Table 2
Parameters in Eqs. (41) and (42)

	Full energy analysis	Convection neglected
C	$-\frac{k_m}{l_m} - \frac{k_d A_a}{1 - \exp(-A_a l_d)}$	$-\frac{k_m}{l_m} - \frac{k_d}{l_d}$
D	$\frac{k_m}{l_m}$	$\frac{k_m}{l_m}$
E	$\frac{k_m}{l_m}$	$\frac{k_m}{l_m}$
F	$-\frac{k_m}{l_m} - \frac{k_d A_c}{\exp(A_c l_d) - 1}$	$-\frac{k_m}{l_m} - \frac{k_d}{l_d}$
G	$-\frac{k_m B_m l_m}{2} + k_d \left[\frac{B_d}{A_a} - \frac{A_a T_0 + B_d l_d}{1 - \exp(-A_a l_d)} \right]$	$-\frac{k_m B_m l_m + k_d B_d l_d}{2} - \frac{k_d T_0}{l_d}$
H	$-\frac{k_m B_m l_m}{2} + k_d \left[-\frac{B_c}{A_c} - \frac{A_c T_0 - B_d l_d}{\exp(A_c l_d) - 1} \right] - S_{\text{reaction}}$	$-\frac{k_m B_m l_m + k_d B_d l_d}{2} - \frac{k_d T_0}{l_d} - S_{\text{reaction}}$
\bar{T}_a	$T_0 + \frac{B_d l_d}{2A_a} + \left(\frac{T_1 - T_0}{l_d} - \frac{B_d}{A_a} \right) \left(\frac{1}{A_a} - \frac{l_d}{\exp(A_a l_d) - 1} \right)$	$\frac{T_0 + T_1}{2} + \frac{B_d l_d^2}{12}$
\bar{T}_c	$T_2 + \frac{B_d l_d}{2A_c} + \left(\frac{T_0 - T_2}{l_d} - \frac{B_d}{A_c} \right) \left(\frac{1}{A_c} - \frac{l_d}{\exp(A_c l_d) - 1} \right)$	$\frac{T_0 + T_2}{2} + \frac{B_d l_d^2}{12}$

$$B = \frac{I^2}{k\sigma} \quad (37)$$

For conduction without convection, the corresponding equations become

$$T = T_i - \frac{B}{2}z^2 + \left[\frac{(T_0 - T_i)}{L} + \frac{BL}{2} \right] z \quad (38)$$

$$\frac{dT}{dz} = -Bz + \frac{(T_0 - T_i)}{L} + \frac{BL}{2} \quad (39)$$

Note that B has the same numerical value in both the anode and cathode diffusers, hence the subscript (d) is used. However, A has different values in the anode and cathode diffusers because different gas mixtures will have different specific heat capacities. Hence, the subscripts (a) and (c) are used.

These results are applied to the three domains of the MEA with continuity of temperature at each interface, and continuous heat flux at the anode catalyst interface. At the cathode catalyst interface where the heat of reaction is generated, the following energy balance applies

$$S_{\text{reaction}} = \left(k \frac{dT}{dz} \right)_{m,2} - \left(k \frac{dT}{dz} \right)_{c,2} \quad (40)$$

The subscripts (m) and (c) refer to the heat transfers through the membrane and cathode regions, respectively, while (2) refers to the position, $\zeta = 2$. Solving, we get

$$T_1 = \frac{FG - DH}{CF - DE} \quad (41)$$

$$T_2 = \frac{CH - EG}{CF - DE} \quad (42)$$

Table 2 shows the expressions for the above constants for two cases: (1) the detailed energy analysis including conduction, convection and ohmic heating, and (2) a simplified energy analysis including conduction and ohmic heating, but neglecting convection.

2.4. Numerical values

The numerical values used in the computation are the same as ref. [3]. The results presented in this paper attempt to simulate the experimental results presented by Wang et al. [4]. Inlet gases were supplied at 150 °C (423 K) and 1 atm. Both fuel (hydrogen) and oxidant (oxygen or air) were humidified at 28 °C. So we assume that the partial pressure of water vapor in the inlet streams is equal to the saturation vapor pressure at 28 °C.

3. Results and discussion

Fig. 2 compares the theoretical IV curve with experimental data for both oxidants, air and oxygen. The analytical results compare well with the experimental data. For the given operating conditions, respective peak power densities of 1.58 and 1.14 kW m⁻² for oxygen and air are predicted.

Fig. 3 shows the maximum temperature increase at different current densities using air as the oxidant. The maximum tem-

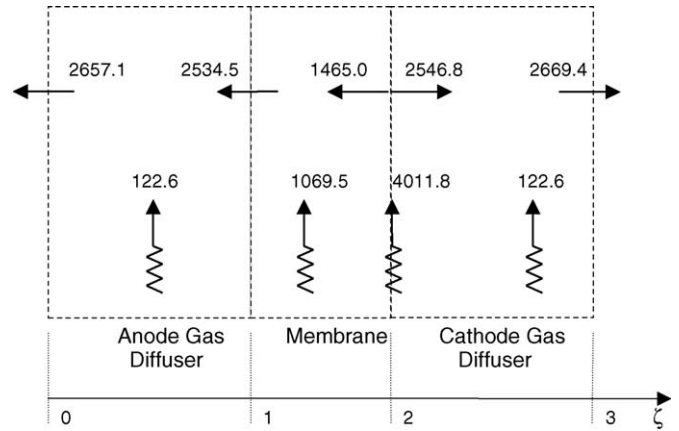


Fig. 4. Thermal balance (W m⁻²) at I = 5000 A m⁻².

perature is expected to occur in the cathode catalyst layer where the heat of reaction is generated. The temperature increase is then defined as T₂ – T₀. This maximum temperature variation increases exponentially with current density, and for the range of current densities shown, is less than 2 K. This value represents the 1D temperature variation in the direction perpendicular to the MEA at any given section. This model does not account for temperature variations in the direction of the gas channels. Depending on the flow rate, the latter variation may be significant.

It can be seen from Fig. 3 that neglecting convection in the energy analysis makes little difference in the temperature variation. Thus, convection is a negligible means of heat transfer in the MEA of PEM fuel cells. Because the solid material is thermally conductive and the fluid velocities are very small, conduction dominates the heat transfer process.

Fig. 4 shows the magnitudes of the heat generations and conduction heat transfers at 5000 A m⁻². Ohmic heating in the membrane is in the same order of magnitude as the heat of reaction, but the ohmic heating in the diffusers are of a smaller order of magnitude. This is due to the high electrical conductivity of the diffuser material, compared to the low ionic conductivity of the PBI membrane.

4. Conclusion

Analytical correlations for intermediate temperature PEMFCs were presented. The correlations are able to accurately predict the polarization effects, since results compare favorably with published experimental data. In addition, a 1D temperature variation of less than 2 K is predicted within the cell for typical operating current densities. The results also suggest that convection is not a significant mode of heat transfer in intermediate temperature PEMFCs.

Acknowledgements

The authors are grateful for the FIU Graduate School Dissertation Fellowship, and to Gas Technology Institute (Contract Number 8390) for their support of this work.

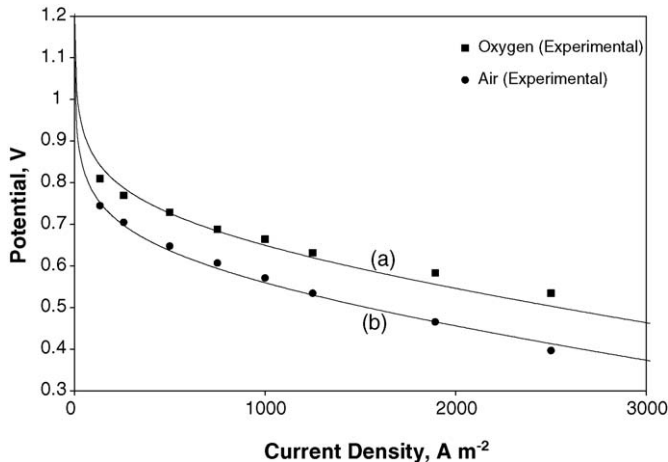


Fig. 2. IV curves for analytical and experimental results. (a) Analytical results for oxidant = oxygen; (b) analytical results for oxidant = air.

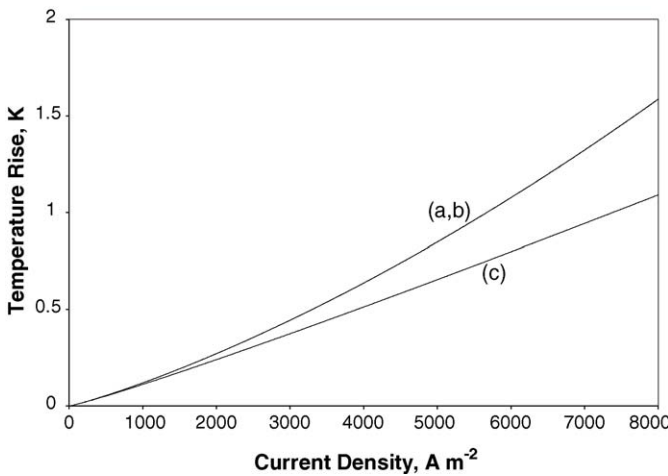


Fig. 3. Maximum temperature rise vs. current density. (a) Conduction, convection and ohmic heating; (b) conduction and ohmic heating with no convection; (c) conduction only without convection and ohmic heating.

References

- [1] O. Savadogo, Emerging membranes for electrochemical systems. Part II. High temperatures composite membranes for polymer electrolyte fuel cell (PEFC) applications, *J. Power Sources* 127 (2004) 135–161.
- [2] D. Cheddie, N. Munroe, Review and comparison of approaches to proton exchange membrane fuel cell modeling, *J. Power Sources* 147 (2005) 72–84.
- [3] D. Cheddie, N. Munroe, Mathematical model of a high temperature PEMFC using a PBI membrane, *Ener. Conver. Manage.*, in press.
- [4] J.T. Wang, R.F. Savinell, J.S. Wainright, M. Litt, H. Yu, A H_2/O_2 fuel cell using acid doped polybenzimidazole as polymer electrolyte, *Electrochim. Acta* 41 (1996) 193–197.